Investigating the Characteristics of a Natural Fiber Composite Fabricated from 9,9'-Bis(aryl)fluorene-modified Nanocellulose and Bamboo Fiber

Khan Md Sefat,[a] Takashi Kurose,[b] Masahiro Yamada,[c] Hiroshi Ito,[d] and Shinichi Shibata [a,*]

A composite fabricated from 9,9'-bis(aryl)fluorene-modified nanocellulose (FCF) and bamboo fiber was studied to explore its processing conditions and limitations. The FCF acted as a binding agent, and bamboo fibers were used as structural reinforcement. Two types of FCF were fabricated and studied: hydroxy and epoxy functional groups with FCF. The FCF solution was homogenized and coated on bamboo fiber sheets. These sheets were laminated with FCF by hot-pressing at various temperatures, pressures, and weight fractions. Flexural modulus and strength were determined at each processing condition. Epoxy type FCF composites exhibited superior flexural performance compared to the hydroxy type. The epoxy type showed better homogeneous dispersion, which increased interfacial area between fibers. The optimal processing temperature was 230 °C. It was considered that thermal degradation occurred above 250 °C and chemical reaction between binder and bamboo was not enough below 210 °C. Flexural performance in the composites showed that approximately 10 MPa was structurally better due to increase of contact area among fibers, which was crushed flat by pressure.

DOI: 10.15376/biores.17.3.4559-4567

Keywords: Bamboo fiber; 9,9'-Bis(aryl)fluorene-modified nanocellulose; Green composite; Flexural properties

*Contact information: a: Faculty of Engineering, Material Processing Laboratory, University of the Ryukyus, Nishihara 903-0213, Okinawa, Japan; b: Department of Mechanical Engineering, Faculty of Science and Technology, Shizuoka Institute of Science and Technology, 2200-2 Toyosawa, Fukuroi, Shizuoka 437-8555, Japan; c: Energy Technology Laboratories, Osaka Gas. Co., Ltd., 6-19-9 Torishima, Konohana-ku, Osaka 554-0051, Japan; d: Department of Organic Materials Science, Graduate School of Organic Materials Science, Yamagata University, 4-3-16 Jonan, Yonezawa, Yamagata 992-8510, Japan; * Corresponding author: shibata@tec.u-ryukyu.ac.jp*

INTRODUCTION

This study explores the performance characteristics and processing conditions of a completely green composite prepared based on previous studies of composite materials (Sefat *et al.* 2021). Cellulosic materials show great promise as cost effective materials in the current global trend. The goal of the present work is to prepare and evaluate structural materials based on the previously developed composite system.

Introduction of nano-fibrillated cellulose-based composites has widened versatile applications for biocomposites, especially in precision technology. Nanocrystalline cellulose, which has features such as nontoxicity and biocompatibility, is an excellent candidate to be applied in new generation drug release systems and scaffolds for tissue engineering (Bhat *et al.* 2017), *etc*. Composites of nanocellulose and carbon particles in the form of fullerene, graphene, carbon nanotubes, nano diamond, and other carbon nanoparticles, such as activated carbon or carbon black (a form of para-crystalline carbon),

which can be further enriched by metallic or ceramic nanoparticles, oxides, carbides, sulphides, polymers, and enzymes, can serve special purposes with advanced features both in biotechnology and industrial applications (Bacakova *et al.* 2020). Potential sectors where cellulose nanofibers present superior efficiency compared to traditional polymer-based materials include the development of supercapacitors (Yuan *et al.* 2019), shape memory devices, biocatalysts, super-insulation, fabrication of high strength anisotropic foams, hydrogen storage devices (Dhar *et al.* 2018), lithium ion batteries (Zhou *et al.* 2018), electrodes for hydrogen evolution reaction (Li *et al.* 2019), actuators (Xu and Hsieh 2019), and heavy duty absorbents capable of extracting heavy metals (Wicklein *et al.* 2015).

Polymers of benzene derivatives, such as zylon (PBO), aramid, and para-aramid (Kevlar), possess high heat resistance, tensile strength, and Young's modulus compared to any other synthetic polymers. The PBO with 5.3 GPa of tensile strength and Young's modulus of 4.5 GPa is known as the strongest and stiffest of commercially available fiber fit to repair and reinforce concrete and masonry structures in externally bonded composite systems (Park *et al.* 2003). Moreover, benzene-based synthetic composites possess low flammability, high ignition delay, low peak heat release rate, and a high oxygen index, offering increased structural integrity (Dittenber and Gangarao 2012). Such a derivative as 9,9′-bis(aryl)fluorine-modified cellulose nanofiber (FCF) was developed by Sugimoto *et al.* (2019). One of the objectives of the current study is to investigate how the new material, with cardo moieties in the structure, acts as a dispersant improving interfacial adhesion in natural fiber composites. Later, two new editions of the material were developed. Green composites were fabricated with these modified nano fibers to explore material and processing characteristics. Previous studies showed that modification of nanocellulose renders better interfacial adhesion in FCF composite compared to composites made from untreated nanocellulose fiber.

EXPERIMENTAL

Materials and Methods

Bamboo was collected from the west local area of Tokushima Prefecture in Japan. Methodology adopted in this study is identical to the experiments in the previous report of Sefat *et al.* (2021). Bamboo culms were selected from the lower part of the plant, which had been below approximately 2 m of the 15 m height. The culms were cut to 5 cm length and 1.0 cm width; both outer and inner dermal layers were peeled off. Pieces together were boiled with 3% NaOH at 120 ℃ for 2 h in an oil bath. After this alkali treatment, the samples were washed with pure water. Sample pieces were then pressed with a heat press machine (Model 180C, Imoto Machinery Co., Ltd., Kyoto, Japan) at several pressures for 1.5 min at 120 ℃ and turned into bamboo fiber sheets of 0.3 to 0.4 mm in thickness. Figure 1 presents pieces of bamboo culms both raw and treated along with a bamboo sheet obtained after pressing. Two types of binders were prepared using FCF. The FCF nanofiber used was of the same material previously reported by Sefat *et al.* (2021). The cellulose nanofibers were modified with epoxy and hydroxy (OH) functional groups as shown in Fig. 2. Hereafter, each modified fiber is called as epoxy type FCF and OH type FCF, respectively. The FCF binders were supplied by Osaka Gas Chemical Co., Ltd. (Osaka, Japan) and their respective chemical structures are shown in Fig. 2. Each binder was adjusted to a dilution of 1:99 (weight ratio) using DI water and mixed using a mechanical homogenizer at 8000 rpm for 20 min to obtain a homogeneous binder suspension.

Fig. 1. Processing of bamboo fibers: (a) culms cut to pieces before and after alkali treatment from left-side; (b) a bamboo sheet after hot-pressing

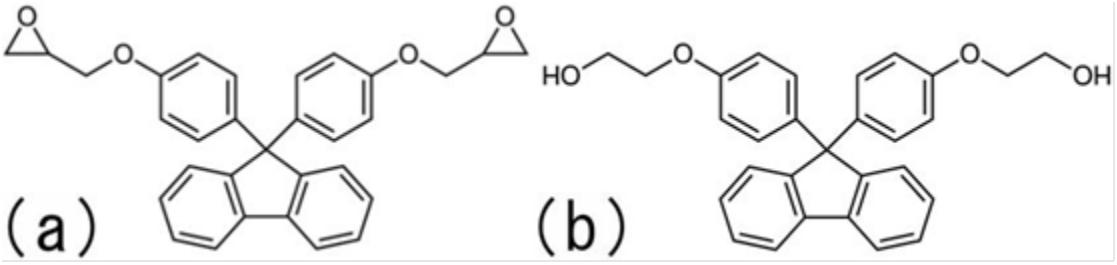

Fig. 2. 9,9′-Bis(aryl)fluorenes with (a) epoxy functional groups and (b) alcohol functional groups

About 10 wt% (with respect to the bamboo fiber mass) of FCF suspensions were poured on the bamboo sheets placed in a stainless steel tray. The samples were then heated in an electric oven at 80 °C for 24 h. Thus, the bamboo sheets were coated with the FCF solution. The three bamboo sheets were placed together unidirectionally and hot-pressed as previously reported (Sefat *et al.* 2021). The synthesis of fluorene-modified CNF (FCF) was described in detail by Sugimoto *et al.* (2019).

Optical photographs were obtained at both the microscale and macroscale levels to observe the structures of fibers and composites. A digital microscope (VHX-950F, Keyence, Osaka, Japan) was utilised to obtain macro-scale visual representation of composite sheet layers. Samples were trimmed to 10 to 12 mm length, and it was then immersed in epoxy resin so that cross-sectional view could be observed. The surface of the specimens where camera lens was focused was polished like a mirror.

The flexural experiment was conducted according to ISO 178 (2019) standard at each condition with three to four specimens using a universal testing machine (Shimadzu EZ Test, Kyoto, Japan). A span length of 22 mm and a crosshead speed of 1.0 mm/min was used in the test. The dimensions of samples used for the flexural testing were prepared as 29 mm in length, 13 mm in width, and 1.0 to 1.65 mm in thickness. The flexural modulus was calculated by the initial derivative line of the load-displacement curve. The maximum inclination line was obtained as the initial derivative line between 0% and 15% of the maximum load. The flexural strength was determined using the maximum load.

Fourier transform infrared (FTIR) spectroscopy was conducted using a Shimadzu IR-Tracer-100 series (Kyoto, Japan) spectrometer by the attenuated total reflectance (ATR) method. Samples were cut to small pieces that fit into a stage of the spectrometer.

RESULTS AND DISCUSSION

Figure 3 shows the flexural modulus and strength values of (a) the 10% epoxy and (b) OH type composites. The epoxy binder incorporated composites exhibited better mechanical properties than that of the OH type binder. The results showed that the OH type had large variation in flexural testing. For the epoxy type, it was found that flexural strength and modulus were highest at 230 to 250 °C. Figure 4 shows the optical microphotographs of the surfaces with (a) a bamboo sheet, (b) the 10 wt% epoxy FCF coated sheet, and (c) 10 wt% OH FCF coated sheet, all hot-pressed at 230 °C for 5 min. The FCF coated area appeared as grey tone in the surfaces. Especially for the OH type, the surface was partially covered by OH binder. The epoxy type FCF suspension was a homogenised mixture in water because of its hydrophobic functional groups. However, the OH type FCF agglutinates each other *via* hydrogen bonds even though homogenized mechanically similar to the epoxy type. Hence, a heterogeneous coating occurred in the OH type. It is considered that this heterogeneous dispersion made gaps while hot-pressing that leads to large variations in the flexural testing as shown in Fig. 3(b).

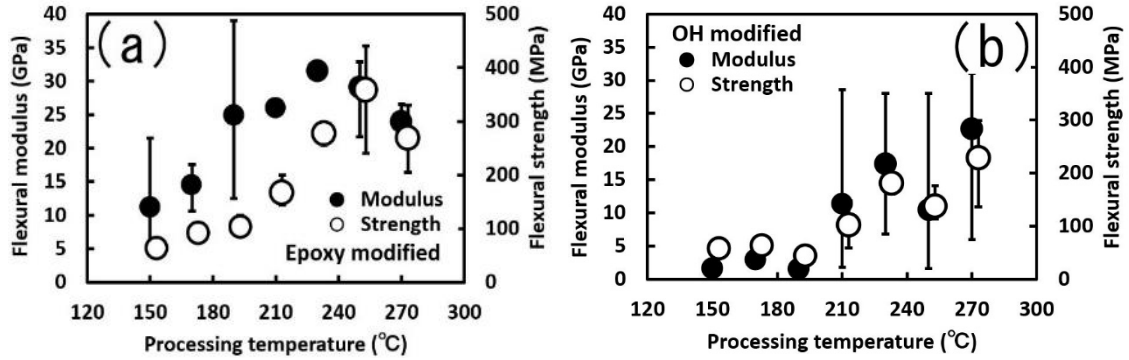

Fig. 3. Flexural modulus and strength values of (a) the epoxy type and (b) OH type FCF-bamboo fiber composites

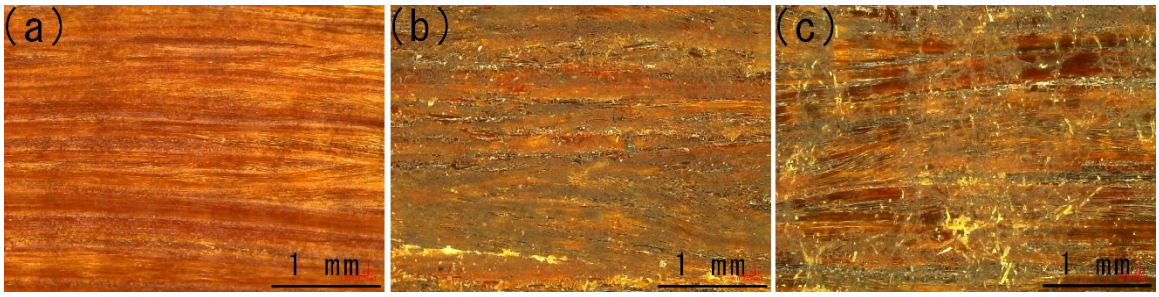

Fig. 4. Optical microphotographs of surfaces with (a) a raw bamboo, (b) epoxy FCF coated sheet, and (c) OH coated sheet

Figures 5(a) and (b) show the ATR spectrum of epoxy and OH type composites before and after hot-pressing at 230 °C, respectively. The intensities of the bands at 3420 cm^{-1} and at 2930 cm^{-1} decreased after hot-pressing. These bands arise due to the stretching vibrations of OH, CH_3, CH_2, and CH groups. The diminishing of these bands can be related to the degradation of hemicelluloses and cellulose. The bands found at 1161 cm^{-1} (C–O–C vibrations in cellulose and hemicelluloses) show the apparent decrease only in epoxy type

composite. Epoxy group is supposed to appear in 910 cm^{-1}; however, no clear change was observed at this wave number in epoxy based FCF. This behaviour suggests the decomposition of hemicellulose. As mentioned above, it is considered that a partial heat conduct occurred because of the gaps in OH type composites without binders. Thus far, the reason for the highest flexural modulus and strength that was observed in Fig. 3(a) is unclear. However, these experimental results suggest that there is an optimum heat temperature for the chemical reaction between binder and bamboo.

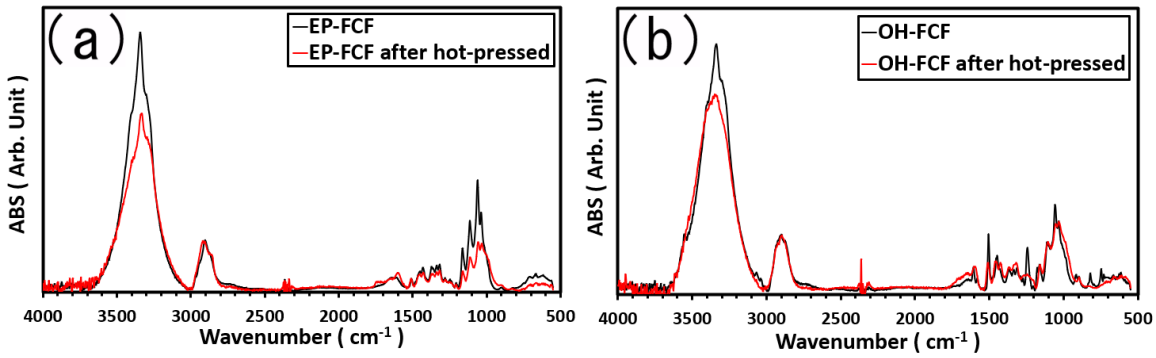

Fig. 5. ATR spectrum of (a) epoxy-based FCF/bamboo composite and (b) OH-based FCF/bamboo composites before and after hot-pressing at 230 °C for 5 min

Figure 6 presents the tensile strength and modulus in single bamboo fibers at various temperatures. The highest values were at 20 °C without any heat treatment. Both strength and modulus decreased gradually with increasing treatment temperature up to 270 °C. Above 300 °C, the mechanical properties decreased dramatically, and tensile testing was not performed. These results agree with the highest values observed approximately at 230 to 250 °C in Fig. 3(a).

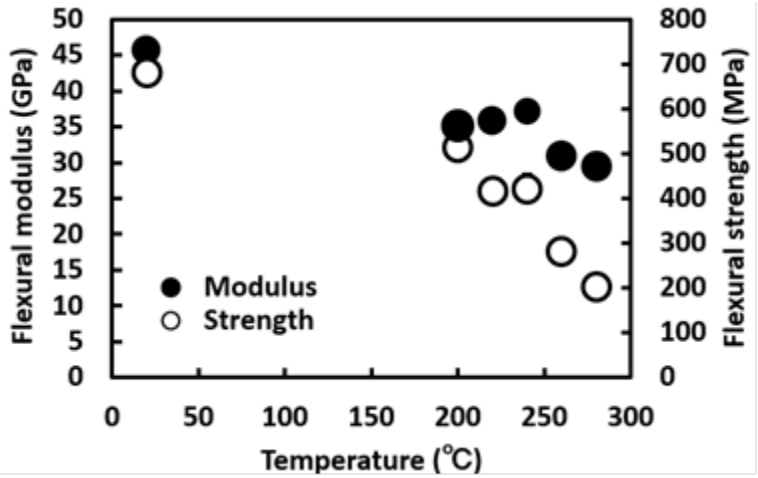

Fig. 6. Relationships between tensile strength and modulus of single bamboo fibers at various temperature

Figure 7 shows the relationships between processing pressure, and flexural strength and modulus of the epoxy type FCF composites at 230 °C for 5 min. Both flexural modulus and strength increased with increasing processing pressure. The highest value was obtained at 10 MPa.

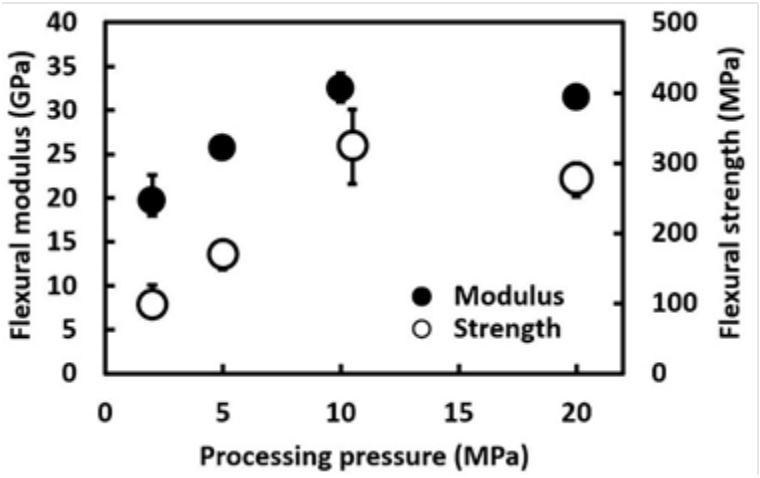

Fig. 7. Relationships between flexural modulus and strength values, and the processing pressures of epoxy-based FCF bamboo composites sheets at 230 °C for 5 min

Figure 8 shows the optical microphotographs of the cross-sectional microstructures of the composites with (a) 2.5 MPa, and (b) 10 MPa. The arc-like shapes shown in Fig. 8 are parts of a metal-made holder to let specimen stand vertically during resin filling in cylindrical mold. There are three layers, corresponding to a single bamboo sheet. The black arrow in Fig. 8(a) indicates solidified epoxy that percolated the composites during embedding in liquid epoxy resin. This means that there was a gap or insufficient interfacial bonding between fibers at 2.5 MPa. The white arrow in Fig. 8(a) indicates the grey colour FCF between bamboo sheets. The thicknesses of each composite were 1020 μm at 2.5 MPa and 780 μm at 10 MPa. For 10 MPa, there were many bamboo bundles crushed flat such as indicated by the black arrow in Fig. 8(b). This deformation increased interfacial area between fibers. This is the reason why flexural properties at the processing pressure at 10 MPa was much higher than that at 2.5 MPa.

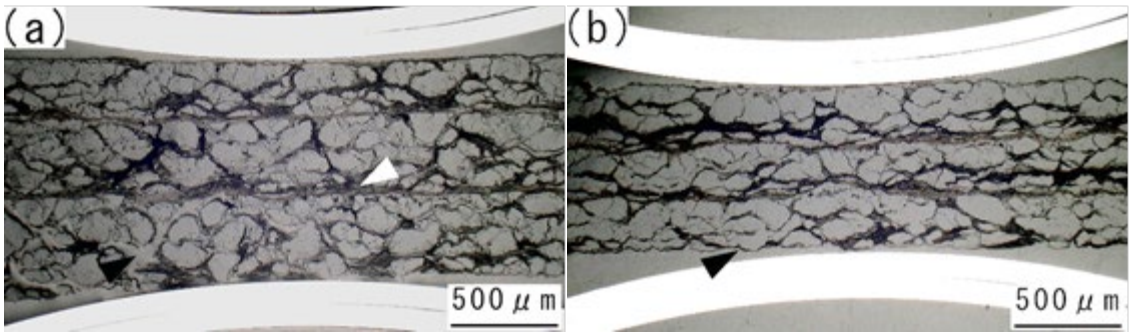

Fig. 8. Optical microphotographs of cross-sectional microstructure in laminated bamboo sheet composites at processing pressure of 2.5 MPa (a) and 10 MPa (b)

Figure 9 shows the relationship between flexural properties and FCF weight percentage in epoxy type bamboo composites. The processing conditions used were pressure of 5 MPa at 230 °C for 5 min. The flexural properties increased with increasing FCF percentage and showed maximum values at 10%.

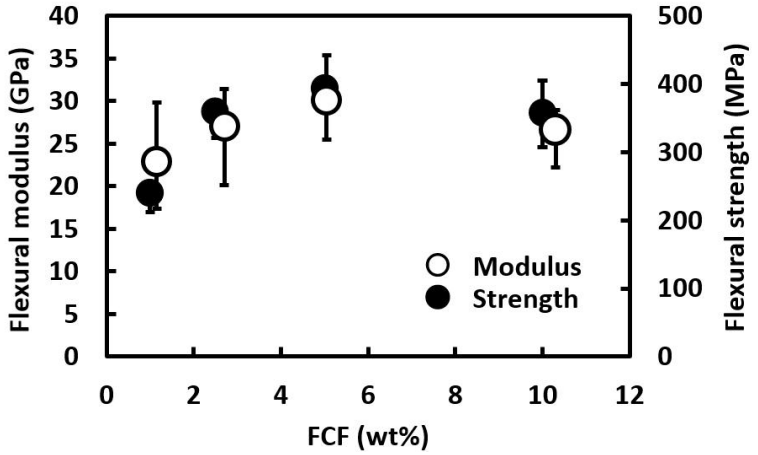

Fig. 9. Relationships between flexural properties at various FCF percentages

Figure 10 shows the optical microphotographs of cross-sectional microstructures of the bamboo composites with (a) 1.0% and (b) 10% FCF. Both microstructures consisted of three sheets. The thickness of each sheet was 780 µm at 1.0% and 796 µm at 10%. The black arrow in Fig. 10(a) indicates epoxy resin that percolated the composites during embedding in liquid epoxy resin, while the white arrow shows the large gap between bamboo sheets. Insufficient binder between bamboo sheets likely caused either case. These gaps and insufficient contact area resulted in weak force transmission in the fiber-reinforced composites. In contrast, the black arrow in Fig. 10(b) indicates a thick FCF-filled gap between bamboo sheets. The presence of this sufficient binder amount in composite seems to increase flexural properties of the composites.

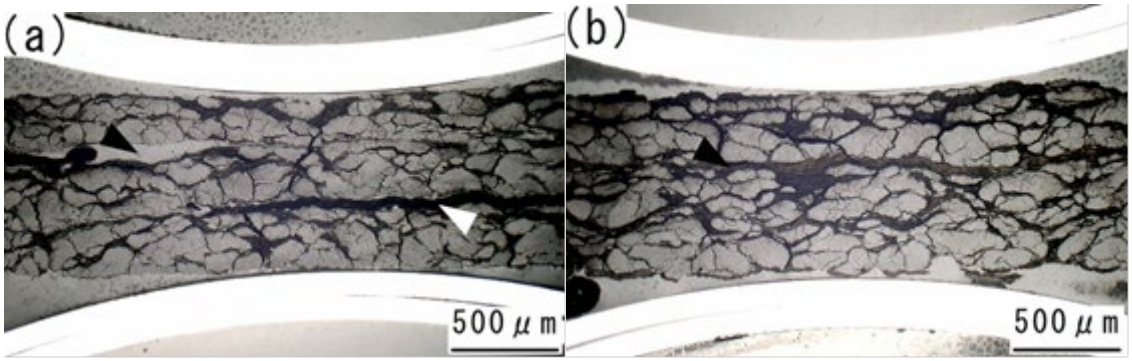

Fig. 10. Optical microphotographs of cross-sectional microstructures of the laminated bamboo sheets composites, (a) FCF percentage at 1.0% and (b) 10.0%

CONCLUSIONS

1. Two types of 9,9'-bis(aryl)fluorene-modified nanocellulose (FCF) derivatives containing epoxy and OH functional groups were used as binders with bamboo sheet composites. The epoxy type showed superior homogeneous dispersion, which was coated on bamboo sheets. The epoxy type FCF covered bamboo sheets thoroughly, and the gap between bamboo sheets was filled to improve interfacial adhesion after hot-

pressing. This homogeneous dispersion resulted in small variation and higher mechanical properties in flexural testing of the composites.

2. Effects of processing temperatures on flexural properties in the bamboo composites were investigated. The highest value was obtained at 230 °C. It was considered that thermal degradation occurred above approximately 250 °C and chemical reaction between binder and bamboo was not enough below 210 °C.
3. The optimal processing pressure and FCF weight percentage was also tested. The optimal pressure was 10 MPa. The bamboo bundles crushed flat at the pressure, increased the interfacial area between fibers, and resulted in higher flexural properties. The highest FCF percentage was 5%. Below 5%, there was insufficient binder between fibers and decreased flexural properties were observed.

REFERENCES CITED

Bacakova, L., Pajorova, J., Tomkova, M., Matejka, R., Broz, A., Stepanovska, J., Prazak, S., Skogberg, A., Siljander, S., and Kallio, P. (2020). "Applications of nanocellulose/ nanocarbon composites: Focus on biotechnology and medicine," *Nanomaterials* 10(2), 1-32. DOI: 10.3390/nano10020196

Bhat, A. H., Dasan, Y. K., Khan, I., Soleimani, H., and Usmani, A. (2017). "Application of nanocrystalline cellulose: Processing and biomedical applications," in: *Cellulose-Reinforced Nanofiber Composites: Production, Properties and Applications*, 215-240. DOI: 10.1016/B978-0-08-100957-4.00009-7

Dhar, P., Gaur, S. S., Kumar, A., and Katiyar, V. (2018). "Cellulose nanocrystal templated graphene nanoscrolls for high performance supercapacitors and hydrogen storage: An experimental and molecular simulation study," *Scientific Reports* 8(1), article no. 3886. DOI: 10.1038/s41598-018-22123-0

Dittenber, D. B., and Gangarao, H. V. S. (2012). "Critical review of recent publications on use of natural composites in infrastructure," *Composites Part A: Applied Science and Manufacturing* 43(8), 1419-1429. DOI: 10.1016/j.compositesa.2011.11.019

Li, G., Yu, J., Zhou, Z., Li, R., Xiang, Z., Cao, Q., Zhao, L., Wang, X., Peng, X., Liu, H., *et al.* (2019). "N-Doped Mo_2C nanobelts/graphene nanosheets bonded with hydroxy nanocellulose as flexible and editable electrode for hydrogen evolution reaction," *iScience* 19, 1090-1100. DOI: 10.1016/j.isci.2019.08.055

Park, J. M., Kim, D. S., and Kim, S. R. (2003). "Improvement of interfacial adhesion and nondestructive damage evaluation for plasma-treated PBO and Kevlar fibers/epoxy composites using micromechanical techniques and surface wettability," *Journal of Colloid and Interface Science* 264(2), 431-445. DOI:10.1016/S0021-9797(03)00419-3

Sefat, K. M., Kurose, T., Yamada, M., Ito, H., and Shibata, S. (2021). "Fabrication of 9,9′-Bis(aryl)fluorene-modified nanocellulose bamboo fiber composite," *BioResources* 16(2), 3907-3915. DOI: 10.15376/biores.16.2.3907-3915

Sugimoto, M., Yamada, M., Sato, H., and Tokumitsu, K. (2019). "Reinforcement of polyamide 6/66 with a 9,9′-bis(aryl)fluorene-modified cellulose nanofiber," *Polymer Journal* 51(11), 1189-1195. DOI: 10.1038/s41428-019-0238-8

Wicklein, B., Kocjan, A., Salazar-Alvarez, G., Carosio, F., Camino, G., Antonietti, M., and Bergström, L. (2015). "Thermally insulating and fire-retardant lightweight anisotropic foams based on nanocellulose and graphene oxide," *Nature*

Nanotechnology 10(3), 277-283. DOI: 10.1038/nnano.2014.248

Xu, X., and Hsieh, Y. L. (2019). "Aqueous exfoliated graphene by amphiphilic nanocellulose and its application in moisture-responsive foldable actuators," *Nanoscale* 11(24), 11719-11729. DOI: 10.1039/c9nr01602c

Yuan, H., Pan, H., Meng, X., Zhu, C., Liu, S., Chen, Z., Ma, J., and Zhu, S. (2019). "Assembly of MnO/CNC/rGO fibers from colloidal liquid crystal for flexible supercapacitors *via* a continuous one-process method," *Nanotechnology* 30(46), article ID 465702. DOI: 10.1088/1361-6528/ab3aaf

Zhou, X., Liu, Y., Du, C., Ren, Y., Li, X., Zuo, P., Yin, G., Ma, Y., Cheng, X., and Gao, Y. (2018). "Free-standing sandwich-type graphene/nanocellulose/silicon laminar anode for flexible rechargeable lithium ion batteries," *ACS Applied Materials & Interfaces* 10(35), 29638-29646. DOI: 10.1021/acsami.8b10066

Article submitted: April 1, 2022; Peer review completed: May 21, 2022; Revised version received: June 2, 2022; Accepted: June 5, 2022; Published: June 13, 2022.
DOI: 10.15376/biores.17.3.4559-4567